CARBON 2019
LEXINGTON, KY

CARBON NANOPARTICLES (CNP) PRODUCTION USING SOLVENT ASSISTED HYDROTHERMAL CARBONIZATION (SA-HTC)

Diego Flores Oña[1*], Andrés Fullana Font[2]

[1]*Affiliation1: Chemical Engineering Faculty, Universidad Central del Ecuador, Quito, Ecuador*
[2]*Affiliation2: Department of Chemical Engineering, Universidad de Alicante, Alicante, Spain*
e-mail: drflores@uce.edu.ec

Introduction

In the last decades, new carbonaceous materials have appeared, they stand out for their excellent physicochemical properties that make them ideal for applications such as: bioimage[1], solar cells[2], ion sensors[3], controlled release of drugs[4], adsorption[5], supercapacitors[6], and photocatalysis[7]. These new materials are the Carbon Nanoparticles (CNP) that can have a spherical, ellipsoidal or tubular shape and within this group are: fullerene, graphene, graphene oxide, nanotubes, nanowires, nanofibers, nanodiamonds, nanospheres, hybrid materials and Carbon Quantum Dots (CQDs).

CNP are high interest because they are non-toxic[8] and have luminescent properties[9] equal to or better than semiconductor nanomaterials based on metals such as cadmium, selenium, tellurium or lead. Also, they are photobleaching resistant and easily water dispersed. They have a chemical surface that can be functionalized, giving them chemical stability, biocompatibility and characteristics to be used as photocatalyst. Its synthesis is relatively easy and cost effective.

Among the production methods of the CNP are the top-down and bottom-up methods, the first one performs the synthesis from carbon structures already formed, while the second one uses simple molecules as precursors to form the structure of the nanoparticles by a polymerization process. Among the top-down methods are: laser ablasion[10], chemical oxidation of arc-discharge[11], electrochemical oxidation[12], and many more. The bottom-up methods are: pyrolysis[13], assisted processes with microwaves[14] and hydrothermal carbonization (HTC)[15].

HTC is one of the most used methods for the synthesis of these nanomaterials, because it performs the process in mild conditions, does not require expensive equipment or reagents, raw materials are abundant, no pre-treatment is required to eliminate moisture and allows the functionalization of its surface[16]. In the regular HTC process, an aqueous solucion with a precursor as a carbon source, is introduced in a closed reactor; it is brought to a certain temperature and time. Three products are generated: a solid carbonaceous material known as hydrochar; a liquid containing soluble substances such as furans, organic acids, aldehydes; and the third product is the CNP that are dispersed in water. A gaseous current also is produced, which is composed of gases such as; CO_2, CO, CH_4 and H_2. The pressure in the reactor is self-generated and the temperatures are in the range of 170 ^oC to 350 ^oC.

The first HTC study to obtain carbonaceous materials was made at the beginning of the 20th century using saccharides as raw material sources. Since then, a lot of research has been carried out with different carbon sources, ranging from simple molecules such as glucose, fructose or sucrose[17], to complex molecules such as starch[18], cellulose[19] and different types of biodegradable biomass of vegetable, animal or industrial origin such as: orange juice[20], banana juice[21], milk[22], human hair[23], among others. Inside the reactor many reactions occur, like; hydrolysis, dehydration,

decarboxylation, and condensation, which can be consecutive or parallel. The principal product of the reactions is 5-(hydroxymethyl) furfural[24,25] (HMF) together with other furans in smaller proportion, these compounds form the hydrochar and the CNP by means of aromatization and polymerization processes. Due to the reaction conditions of the process, temperature gradients are formed, which together with the HMF, furans and gases create environments that make it difficult to control the characteristics of the final product. As a consequence of this, a lot of products were generated during the polymerization process. The chemistry of furans is very extensive, and many possible reactions can occur simultaneously with a heterogeneous system like the hydrothermal process.

Once the HTC process has finished, one of the fundamental steps is the separation of the products. The hydrochar can be separated from the aqueous solution by simple filtration, while to separate the CNP there are different methods such as: electrophoresis with polyacrylamide gel, dialysis, centrifugation or extraction with solvents. In the last method the aqueous solution is mixed with an organic solvent that is immiscible with water and due to the polarity effect, the CNP will migrate from the water to the organic solvent. In our study we call this process solvent extraction hydrothermal carbonization (SE-HTC). It has been supposed that, if the organic solvent together with water were introduced in the reactor, the reaction conditions would change, resulting in carbonaceous materials with different characteristics, and the variation of the mass yield. The process, where a blend of organic solvent-water is used in the hydrothermal process, is called; solvent assisted hydrothermal carbonization (SA-HTC). For this purpose, glucose was used as carbon source, using organic solvents of different polarity: hexane, toluene and butyl acetate in the extraction process as well as in the assisted process, in order to determine the characteristics of the final products.

Materials and Methods

Chemicals: D-(+)-Glucose, butyl acetate, hexane and toluene were obtained from commercial sources. Distilled water was used for all the experiments.

Synthesis:

HTC: Dissolve 10 g of glucose in 300 mL of distilled water. The solution is placed in a stainless-steel reactor of 500 mL capacity. It is heated to 200 oC for 4 hours, then the reactor is cooled down, and the hydrochar is separated by filtration, using a membrane filter of 0.45 um. The suspension is ultra-centrifuged for a time of 15 minutes at 20000 rpm, then the liquid is evaporated in a rotary evaporator and finally the CNP are dried in a lab oven for two hours.

SE-HTC: Dissolve 10 g of glucose in 300 mL of distilled water. The solution is placed in a stainless-steel reactor of 500 mL capacity. It is heated to 200 oC for 4 hours, then the reactor is cooled down, and the hydrochar is separated by filtration, using a membrane filter of 0.45 um. The suspension is mixed with 100 mL of organic solvent (hexane, toluene or butyl acetate), which is let to repose for 10 minutes, and the aqueous phase is separated from the organic phase, each of the fractions is ultra-centrifuged for a time of 15 minutes at 20000 rpm, then the liquid is evaporated in a rotary evaporator, and finally the CNP from the aqueous phases and those derived from the organic phase are dried in a lab oven for two hours.

SA-HTC: Dissolve 10 g of glucose in 300 mL of distilled water, add 100 mL of organic solvent (hexane, toluene or butyl acetate) and place the solution into a stainless-steel reactor of 500 mL capacity. It is heated to 200 ^{o}C for 4 hours, then the reactor is cooled down, and the hydrochar is separated by filtration, using a membrane filter of 0.45 um. Repose the blend for 10 minutes, the aqueous phase is separated from the organic phase, each of the fractions is ultra-centrifuged for a time of 15 minutes at 20000 rpm, then the liquid is evaporated in a rotary evaporator, and finally the CNP from the aqueous phases and those derived from the organic phase are dried in a lab oven for two hours.

***Characterization methods*:** FESEM images were obtained by using a Carl Zeiss microscope. TEM images were taken using a TEM-200 microscope operating at 200 kV. Fourier transform infrared spectra of the materials in powder form were analyzed using a Perkin Elmer Spectrum Two FT-IR Spectrometer. The elemental analysis (C, H, and O) was performed using an ELEMENTAR VARIO CUBE Analyzer. Absorption spectra were made on Cary 60 UV-Vis Spectrophotometer. Emission spectra were measured with BioTek Synergy H1 spectrometer.

Results and Discussion

In both process: SE-HTC and SA-HTC; there are three solid products: the hydrochar, the CNP of the organic phase, and the CNP of the aqueous phase, the mass yield of these products are in table 1, the total yield is the sum of the three solid products that were generated in the process.

Table 1. Mass yields from SE-HTC and SA-HTC processes

Process	Solvent	Time of reaction (h)	Mass Yield (%)			
			Hidrochar	CNP Organic phase	CNP Aqueous phase	TOTAL
HTC	---	4	16,88	0	32,01	48,89
SE-HTC	Hexane	4	14,81	0,38	36,44	51,63
	Toluene	4	15,93	1,48	33,40	50,81
	Butyl Acetate	4	14,11	3,89	35,99	53,99
SA-HTC	Hexane	4	10,94	2,13	37,25	50,32
	Toluene	4	8,38	3,86	39,06	51,33
	Butyl Acetate	4	1,74	14,11	32,51	48,35
		2	1,59	15,07	32,38	49,04
		1	5,62	13,95	30,14	49,71

For the three processes: HTC, SE-HTC and SA-HTC, there is a total mass yield of around 50% in all samples, regardless of the type of process or the type of solvent used. The total mass yield is within the range of solid products (50% to 80%) obtained in a common hydrothermal carbonization process as mentioned by Libra, Ro, Kammann[26] et al. Therefore, using a blend of organic solvent-water in the process instead of only water does not affect the total yield of carbonaceous material that is produced. But, in all cases the mass distribution of the hydrochar and the CNP of the aqueous phase and the organic phase is different. The amounts of hydrochar obtained in the SA-HTC processes are lower than the hydrochar obtained in the SE-HTC processes, on the contrary; for the

CNP, the mass yield increases when SA-HTC process takes place. When an organic solvent is introduced in the reactor, the precursor tends to form CNP instead of forming hydrochar and this phenomenon is greater when the polarity of the solvent increases (polarity index: hexane 0.0 toluene 2,4, butyl acetate 3,9, water 9,0). In this way, with butyl acetate the highest amount of CNP was obtained, and the lowest amount of hydrochar. This solvent was tested at different reaction times, 1, 2 and 4 hours, the CNP mass yield at all times is very similar, around 14%. Therefore, the mass of products generated in the SA-HTC process depends on the organic solvent, but not on the reaction time.

One posible reason for the formation of higher amount of CNP and lower amount of hydrochar in the SA-HTC process is described by Kuster[24], who mentions that HMF can be hydrolyzed by taking two molecules of water from the medium to become levulinic acid and formic acid. Hence, if the HMF is not in the aqueous medium, but in an organic phase, its hydrolysis would be avoided and there would be a greater amount of HMF. In this case, during the SA-HTC process, the HMF would pass from the aqueous phase to the organic phase, hydrolysis would be prevented, and the aromatization and polymerization reactions would occur with a tendency to form CNP instead of hydrochar.

Despite determining the mass yield of the solid products in the HTC, SE-HTC and SA-HTC processes, the carbonaceous materials that is of interest are the CNP that are in the organic phase.

Table 2. Elemental Analysis of CNP obtained in SE-HTC and SA-HTC processes

Process	Solvent	Time of reaction (h)	Sample code of CNP	C (wt%)	H (wt%)	O (wt%)	O/C*	H/C*
--	--	--	Glucose	40,00	6,67	53,33	1,00	2,00
HTC	--	4	G1	46,79	7,31	45,90	0,74	1,87
SE-HTC	Hexane	4	SE1	47,85	6,09	46,06	0,72	1,53
	Toluene	4	SE2	54,13	6,90	38,97	0,54	1,53
	Butyl Acetate	4	SE3	60,93	5,48	33,59	0,41	1,08
SA-HTC	Hexane	4	SA1	52,71	6,52	40,77	0,58	1,48
	Toluene	4	SA2	53,08	6,57	40,35	0,57	1,49
	Butyl Acetate	4	SA3	63,78	6,37	29,85	0,35	1,20
		2	SA3[a]	64,68	5,48	29,84	0,35	1,02
		1	SA3[b]	65,14	4,89	29,97	0,35	0,90

*Atomic ratios

Table 2 shows the elemental analysis of the CNP obtained in all hydrothermal carbonization processes. Regardless of the type of process (SE-HTC or SA-HTC), the amount of C increases, while the amount of O decreases, and in the case of H it remains mostly constant. In both processes , there is an influence of the organic solvent, when the polarity increases, higher carbon percentages are reached, and in some cases, up to 60% of C was reached , just like in research carried out by Karak[21]. On the other hand, the percentage of oxygen decreases as the polarity of the solvent increases, which implies that the number of oxygenated groups decreases as the polarity index of the organic solvent is higher. With the percentages obtained, the atomic ratios; O/C and H/C were

determined, these data are located in the Ven Krevelen diagram where the type of reaction that occurred in the HTC process can be observed (figure 1).

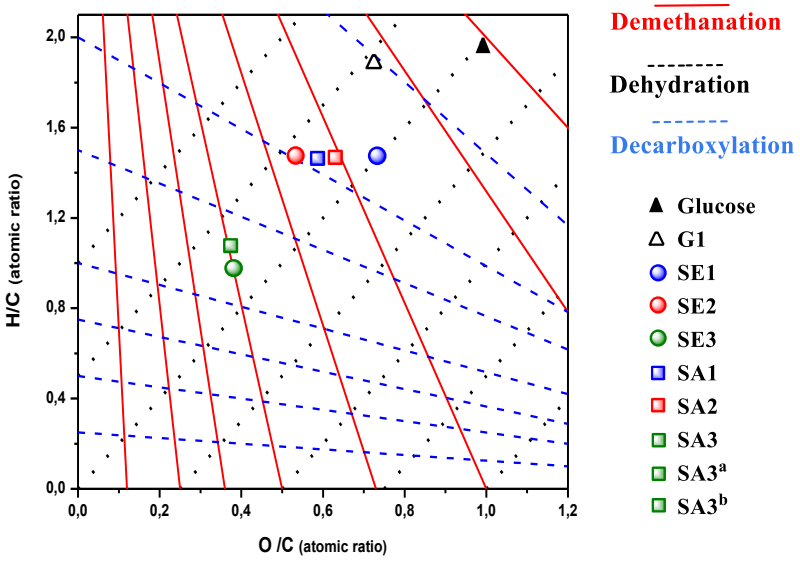

Figure 1. Venn Krevelen diagram for samples of the SE-HTC and SA-HTC processes

Regardless the process being SE-HTC or SA-HTC, the reaction that governs the processes is dehydration, followed by decarboxylation, and for both processes demethanation does not take place. When butyl acetate is used as solvent, greater dehydration is achieved compared to the other solvents; therefore, there is an effect of polarity on the degree of dehydration. On the other hand, at any reaction time (1, 2 and 4 hours), there is no significant difference in the atomic ratio obtained, therefore; time does not affect the dehydration of the precursor.

The changes in the chemical structures of the samples after the HTC process have been analyzed using FT-IR spectroscopy (Figure 2) and compared with its precursor, glucose.

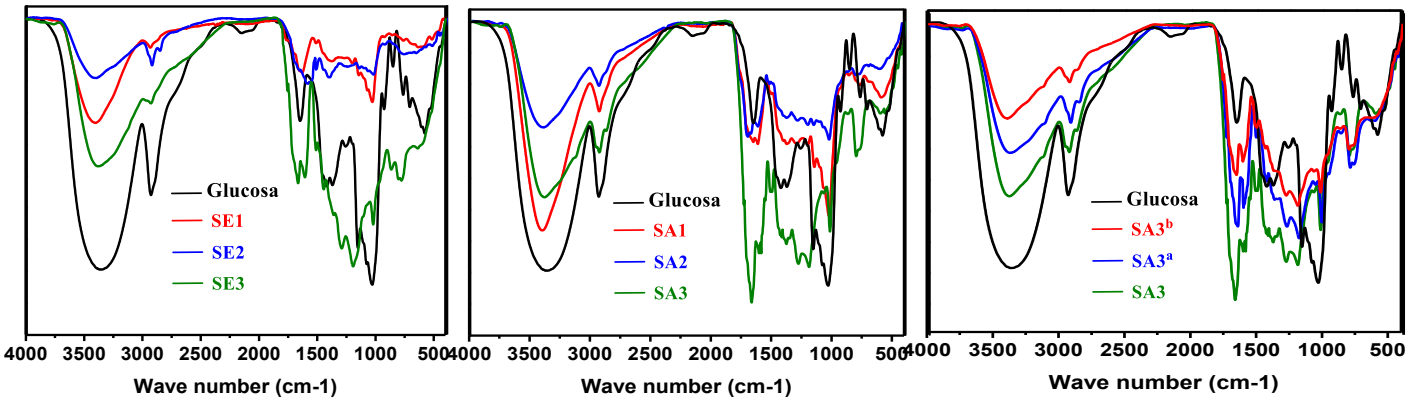

Figure 2. Infrared spectra for the CNP of SE-HTC and SA-HTC processes

The band at 3370cm^{-1} corresponds to the O-H group (hydroxyl), the band at 2995cm^{-1} to C-H groups (aliphatic), while the band at 1650cm^{-1} is attributed to C=O (carbonyl and quinone) and the 1395cm^{-1} band to C=C (aromatics), the band of 1046cm^{-1} is for C-O-C/ C-O groups (hydroxyl,

ester, ether) and finally band 844cm^{-1} to C-H (aromatics).

In all the CNP of the SE-HTC and SA-HTC processes, the intensity of the bands corresponding to the hydroxyl group (3370cm^{-1}), is weaker than the band of glucose. A decrease in the bands of the C-H groups (aliphatic) and an increase of the C=C and C-H (aromatics) bands is also observed. Considering that the O-H group is the lost group in dehydration and that the CNP are aromatic and non-linear systems, the results of the Ven Krevelen diagram confirm that the dehydration and aromatization take place during the HTC processes.

The carbonyl group (C=O) (one of the oxygenated groups that gives polarity to the CNP), has a different behavior, for the samples SE1 and SE2 the band decreases, while for samples SA1 and SA2 the band remains mostly constant, these four samples were made with hexane and toluene respectively, which are the solvents with the lower polarity. In contrast, for samples SE3, SA3, SA3^{a} and SA3^{b} that were treated with butyl acetate, the intensity of the C=O band increases significantly; a similar case happens with the bands of groups C-O-C/C-O. The latter is expected, since butyl acetate has a greater polarity than toluene and hexane, and it will draw CNP that have more oxygenated polar groups (hydroxyl, carbonyl and carboxyl) in their chemical structure.

In the research conducted by Titirici[27] et. al., the synthesis of carbon nanodots was made from glucose, similar to the procedure performed in this study. One of the conclusions from TEM images, is that the product of the reaction is a heterogeneous mixture of amorphous-like, carbon-black type and various crystalline nanoparticles including carbon onions and expanded nanographite. On the other hand, the research carried out by Tang[28] et. al. also observed in the TEM images, a mixture of dispersed particles and amorphous CQD in the range of 2 to 6 nm. In this case, a similar result is recognized since the TEM and FESEM images (figure 3) indicate that there is a spherical CNP mixture with different sizes, along with amorphous carbonaceous material. In addition, very small amounts of CQD were observed. For sample G1, the size distribution is from 25 nm to 124 nm. The ultra-centrifugation that is performed on the samples treatment is fundamental for the process, because if it´s not actioned, a large amount of carbonaceous material is observed in the TEM and FESEM images, which prevents proper observation of the nanospheres.

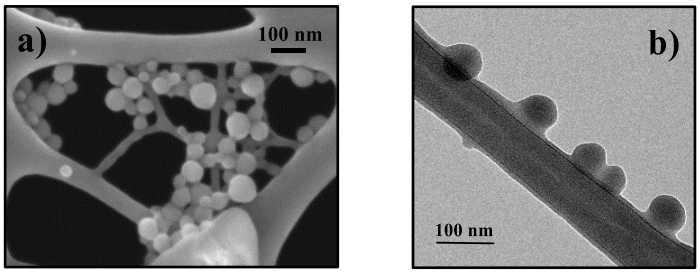

Figure 3. a) FESEM image for sample G1, b) TEM image for sample SE3

Although the TEM and FESEM used provide high resolution, the images are difficult to capture, due to, the low contrast that exists between the CNP and the carbon coated grids of the microscopes. Furthermore, when the electron beam of the equipment impinges on the nanoparticles, they become electrically charged and move or reflect light, which makes it challenging to obtain an image[27].

As mentioned above, one of the issues in the HTC is the high heterogeneity of the process, for that, the extraction with solvents (SE-HTC) allows to separate the nanoparticles and classify them according to their chemical affinity. In this research, the separation was carried out with three solvents: hexane, toluene, and butyl acetate. In the TEM and FESEM images of samples SE1 and SE2, a small amount of nanospheres is observed in a matrix of amorphous carbonaceous material; but in sample SE3 (figure 3b) a high number of nanoparticles with diameters ranging from 34 nm to 122 nm is observed. Comparing samples SE3 and G1, both have very much alike range of diameters that are highly dispersed, but the polarity of the nanospheres is different, therefore, it can be stated there is no relationship between polarity and the size of the nanoparticles, thus, the nanoparticles can be either large or small and have the same surface chemistry.

In the SA-HTC process, a similar situation to the SE-HTC process occurs, for the SA1 and SA2 samples the TEM and FESEM images show small amounts of nanospheres in a matrix of amorphous carbonaceous material, while in the samples SA3^{b}, SA3^{a} and SA3, a great quantity of nanospheres is observed (figure 4), with size range of 56 nm to 290 nm, 83 nm to 268 nm, and 80 nm to 275 nm, respectively. Once more, the particles display high dispersion size, but the range remains mainly constant despite the different reaction times, therefore; time does not influence the size of the nanoparticles.

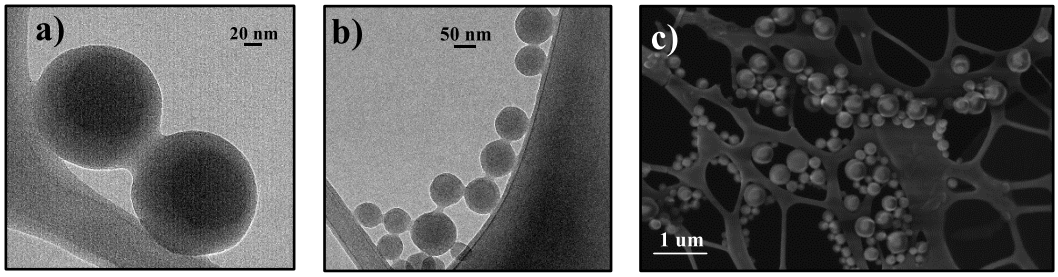

Figure 5. a) TEM image of sample SA3, b) TEM image of sample SA3^{a}, c) FESEM image of sample SA3^{b}

One of the most important characteristics of the CNP is their optical properties. Figure 6a shows the absorption spectrum of all the samples of the hydrothermal carbonization processes, all spectra have a peak at 280 nm in the ultraviolet region with a tail that extends along the visible region. Moreover, there is another peak at 327 nm with low intensity. According to the analysis of microscopy and FT-IR, the samples are a mixture of nanospheres of different sizes and with different functional groups in their structure. However, every absorption spectrum are equal, which implies that the absorbance in the spectra is attributed to transitions π-π^* of the carbon double bonds (C=C) of the aromatic compounds that are present in the nanospheres. There is hardly any influence of n-π^* transitions that produce C=O bonds that are on the surface of CNP. Hence, neither the size nor the functional groups on the surface of the nanoparticles present influence in the absorption spectrum.

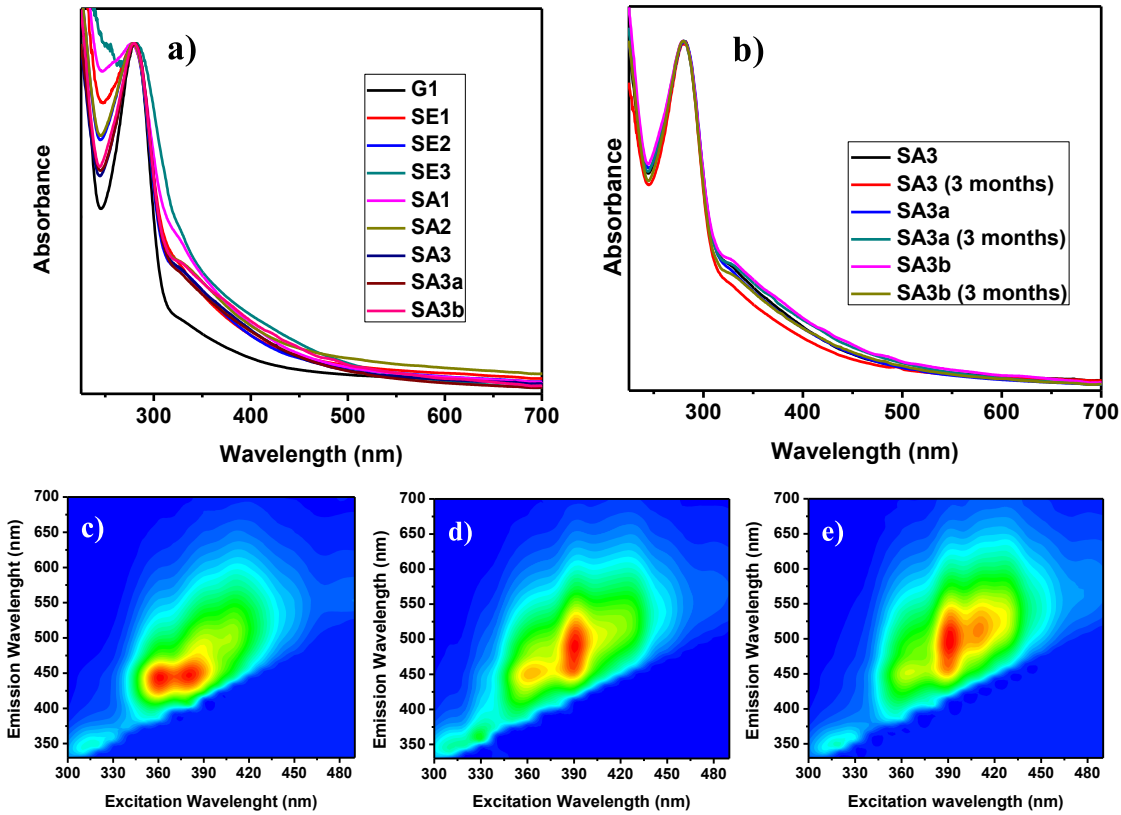

Figure 6. a) Absorption spectra for samples from SE-HTC and SA-HTC processes, b) Absorption spectra for the samples treated with butyl acetate at different storage times, c) PL map for the sample G1 d) PL map for sample SA3, e) PL map for sample SA3 stored for three months

The nanospheres present a high photoluminescence (PL) that is dependent on excitation. Figure 6c shows a PL map for the sample G1, obtained from the compilation of the emission spectra, taken at different excitation wavelengths, from 300 nm to 490 nm with 10 nm intervals. There are two zones with a maximum fluorescence intensity, one at 345 nm corresponding to the blue color and another at 495 nm corresponding to the green color. Any SE-HETC and SA-HTC samples, have a PL map equal to the G1 sample, this is why all diagrams are not shown in this article. Thus, the emission phenomenon is a product of the aromatic structure of the nanospheres and does not depend on the particle size nor the surface functional groups, as it was already acknowledged in the absorption spectra.

Since the CNP treated with butyl acetate present higher yield, samples SA3, SA3^{a} and SA3^{b} were stored for three months without protecting them from light. The absorption spectrum and the PL map were achieved (Figure 6b, 6d and 6e), with obtaining peaks of absorption and fluorescence intensity equal to the storageless samples. In addition, new peaks were not observed, which indicates that the samples are photo-stable and do not lose their optical characteristics over time.

Conclusions

The amount of total solid products that are generated in an HTC process does not depend on the liquid used in the process. Whether water or a blend of water-organic solvent is placed inside the reactor, the total yield does not vary. However, the amount of CNP that are in the aqueous phase and in the organic phase does differ if the process is extraction or assisted. The best performance of CNP is in the SA-HTC process with butyl acetate as the organic solvent. In addition, these results do not alter with the reaction time. Hence, at different times the amount of CNP obtained remains mainly constant. In the SA-HTC process with butyl acetate, regardless of the reaction; the highest degree of dehydration was achieved according to the Ven Krevelen diagram and the FT-IR spectra. When it comes to the optical properties, the C=C aromatic functional groups are those that govern the processes of absorption and emission light. In both SE-HTC and SA-HTC processes, the optical properties do not depend on the synthesis conditions. Even though the CNP had already been processed several months ago, their optical properties remain the same.

Acknowledgment

This work has been carried with the financial support of Universidad Central del Ecuador

References

1. Ray, S. C., Saha, A., Jana, N. R., & Sarkar, R. (2009). Fluorescent Carbon Nanoparticles : Synthesis, Characterization , and Bioimaging Application, *J. Phys. Chem. C* 113, 18546–18551.
2. Young, T., Alegaonkar, P. S., & Yoo, J. (2007). Fabrication of dye sensitized solar cell using TiO 2 coated carbon nanotubes, *Thin Solid Films* 515, 5131–5135.
3. Guo, Y., Zhang, L., Zhang, S., Yang, Y., Chen, X., & Zhang, M. (2015). Biosensors and Bioelectronics Fluorescent carbon nanoparticles for the fl uorescent detection of metal ions. *Biosensors and Bioelectronic* 63, 61–71.
4. Oh, W., Yoon, H., & Jang, J. (2010). Biomaterials Size control of magnetic carbon nanoparticles for drug delivery. *Biomaterials* 31(6), 1342–1348.
5. Pan, B. O., & Xing, B. (2008). Critical Review Adsorption Mechanisms of Organic Chemicals on Carbon Nanotubes, 9005–9013.
6. Zhi, M., Xiang, C., Li, J., Li, M., & Wu, N. (2013). Nanostructured carbon – metal oxide composite electrodes for supercapacitors : a review, *Nanoscale* 5, 72–88.
7. Cao, L., Sahu, S., Anilkumar, P., Bunker, C. E., Xu, J., Fernando, K. A. S., … Sun, Y. (2011). Carbon Nanoparticles as Visible-Light Photocatalysts for Efficient CO 2 Conversion and Beyond, *JACS* 133, 4754–4757
8. Fiorito, S., Serafino, A., Andreola, F., Togna, A., & Togna, G. (2006). Toxicity and Biocompatibility of Carbon Nanoparticles, *Journal of Nanoscience and Nanotechnology* 6(3), 591–599.
9. Li, H., He, X., Liu, Y., & Kang, Z. (2010). One-step ultrasonic synthesis of water-soluble carbon nanoparticles with excellent photoluminescent properties. *Carbon* 49(2), 605–609.
10. Chen, G. X., Hong, M. H., Chong, T. C., Elim, H. I., Ma, G. H., Chen, G. X.,(2004). Preparation of carbon nanoparticles with strong optical limiting properties by laser ablation in water, *J. Appl. Phys.* 95, 1455, 1–6.
11. Datsyuk, V., Kalyva, M., Papagelis, K., Parthenios, J., Tasis, D., Siokou, A.,Galiotis, C. (2008). Chemical oxidation of multiwalled carbon nanotubes, *Carbón*, 46, 2–9.
12. Lu, J., Yang, J., Wang, J., Lim, A., Wang, S., & Loh, K. P. (2009). One-Pot Synthesis of Fluorescent Carbon Graphene by the Exfoliation of Graphite in Ionic Liquids, *ACSNano* 3(8), 2367–2375.
13. Clinard, C. (2002). Carbon nanoparticles from laser pyrolysis, *Carbon* 40, 2775–2789.
14. Chandra, S., Das, P., Bag, S., Laha, D., & Pramanik, P. (2011). Synthesis, functionalization and bioimaging applications of highly fluorescent carbon nanoparticles, *Nanoscale* 3, 1533–1540.
15. Titirici, M.-M., & Antonietti, M. (2010). Chemistry and materials options of sustainable carbon materials made by hydrothermal carbonization. *Chem. Soc. Rev* 39(1), 103–116.
16. Sevilla, M., & Fuertes, A. B. (2009). Chemical and Structural Properties of Carbonaceous Products Obtained by Hydrothermal Carbonization of Saccharides, Chem. Eur. J. 15, on4195–4203.

17. van Dam H. E., Kieboom A. P. G., van Bekkum H. (1986), The Conversion of Fructose and Glucose in Acidic Media: Formation of HydroxymethylfurFuraI, *Starch* 38, 95–101.
18. Fun, S., Nur, S., Mohd, A., Cem, S., & Muk, S. (2012). Facile synthesis of fluorescent carbon nanodots from starch nanoparticles. *Materials Letters* 85, 50–52.
19. Sevilla, M., & Fuertes, A. B. (2009). The production of carbon materials by hydrothermal carbonization of cellulose. *Carbon* 47(9), 2281–2289.
20. Sahu S., Behera B., Maiti T. K., Mohapatra S., (2012), Simple one-step synthesis of highly luminescent carbon dots from orange juice: application as excellent bio-imaging agents, *Chem. Commun* 48, 8835–8837
21. De, B., & Karak, N. (2013). A green and facile approach for the synthesis of water soluble fluorescent carbon dots from banana juice. *RSC Advances* 3(22), 8286.
22. Zhang, H., Zhang, J., Xie, Y., Liu, L., Wang, H., Tang, Y. (2013). Fabrication, Gradient Extraction and Surface Polarity-Dependent Photoluminescence of Cow Milk-Derived Carbon Dots, *RSC Advances* 00, 1-3
23. Sun, D., Ban, R., Zhang, P., Wu, G., Zhang, J., & Zhu, J. (2013). Hair fiber as a precursor for synthesizing of sulfur- and nitrogen-co-doped carbon dots with tunable luminescence properties. *Carbon* 64, 424–434.
24. Kuster, B. F. M. (1990). 5-Hydroxymethylfurfural (HMF). A Review Focussing on its Manufacture*, *Starch* 42(8), 314–321
25. Teong, S. P., Yi, G., & Zhang, Y. (2015). Hydroxymethylfurfural production from bioresources : past , present and future, *Green Chem* 16, 2015–2026.
26. Titirici, M., Fühner, C., Bens, O., Kern, J., & Emmerich, K. (2011). Hydrothermal carbonization of biomass residuals : a comparative review of the chemistry , processes and applications of wet and dry pyrolysis, *Biofuels* 2(1), 71–106
27. Papaioannou, N., Marinovic, A., Yoshizawa, N., Goode, A. E., Fay, M., Khlobystov, A., Sapelkin, A. (2018). Structure and solvents effects on the optical properties of sugar- derived carbon nanodots. *Scientific Reports* 8, 1–10.
28. Zhang, Z., Hao, J., Zhang, J., Zhang, B., & Tang, J. (2012). Protein as the source for synthesizing fluorescent carbon dots by a one-pot hydrothermal route. *RSC Advances* 2(23), 8599.